TERAHERTZ-FREQUENCY SPECTROSCOPY AS A TECHNIQUE FOR THE REMOTE DETECTION OF BIOLOGICAL WARFARE AGENTS

D.L. Woolard[1]*, E. R. Brown[2], A. C. Samuels[3], T. Globus[4], B. Gelmont[4], and M. Wolski[5]

[1] Army Research Laboratory, Army Research Office, Research Triangle Park, NC
[2] University of California at Los Angeles, Los Angeles, CA
[3] Edgewood Chemical and Biological Center, Aberdeen Proving Ground, MD
[4] University of Virginia, Charlottesville, VA
[5] Naval Surface Warfare Center, Dahlgren, VA

ABSTRACT

This paper discusses the potential use of terahertz-frequency spectroscopy as a technique for the remote detection of biological warfare agents. Here, design studies are presented for a differential-absorption-radar (DAR) approach that utilizes the spectral signatures of *Bacillus (B.) subtillus* spores within the terahertz (THz) regime as the detection mechanism. The signature data used in these studies is taken from laboratory measurements performed on uniform thin films of *B. subtillus* spores and the system performance is assessed for both incoherent and coherent detector modalities. These studies consider DAR remote sensing of biological (bio) clouds at significant ranges (i.e., 1 km) and include the effects of realistic atmospheric conditions. Specifically, THz spectral signatures were used in a high-level remote-sensor design to estimate the probabilities of detection (P_d) and false-alarm (P_{fa}) associated with this general technique. The system design studies suggest useful remote-detection performance can be achieved (i.e., $P_d > 0.9$ & $P_{fa} << 10^{-4}$ for bio-cloud densities $< 10^3$ cm^{-3}) at 1 km ranges if the THz signature information remains predictably stable under varying atmospheric conditions (e.g., changes in humidity, spore activity state, etc). Hence, this paper will also present recent results from scientific studies on bio-molecules that are exploring the underlying mechanisms responsible for the spectral signatures. DAR system performance is also assessed in a more practical bio-warfare military or civilian defense scenario. Here, the P_d and P_{fa} statistics for the DAR system are mapped onto the time-dependent evolution of an aerosol bio-cloud release to give a real-time indication of the effectiveness of the detection methodology. All together, these results demonstrate that standoff detection of bio-agents is feasible for threat-level concentrations in practical battlefield environments at sufficient ranges to provide for early warning.

1. INTRODUCTION

The past and ongoing proliferation of chemical and biological (CB) agents as instruments of warfare and terrorism has elevated the task of developing an adequate civilian and military defense to CB threats to a very high priority. The particular seriousness of this type of threat was emphatically underscored when the leaders of our nation (i.e., both the President and Congress) just recently endorsed a military intervention into Iraq to, if necessary, forcibly neutralize all nuclear and CB warfare capabilities. In the event that our military forces or civilian population faced such threats in the future, an adequate defense would necessitate the ability to rapidly detect and identify both known and unknown threat-agents. Clearly, the most serious threat of CB agents is the potential harm they present to the short and long-term health of the victim(s). However, the actual or perceived threat of CB warfare agents can impact the operational capability of a military force in the field and the productivity of the private sector even when conventional counter-measures (i.e., protective equipment and clothing) are successfully employed. This is true because protective equipment can interfere with vision, speech intelligibility, personal recognition and dexterity. For these reasons, the development of reliable approaches for the detection and identification of CB agents in the field of operation, and within our homeland, is imperative. While much work remains to improve overall sensing capabilities for both chemical and biological agents (Woolard et al., 2000), the present standoff detection (and therefore also identification) techniques for biological (bio) warfare agents are very limited. In fact, the development of a bio early-warning capability is of the *highest priority* to the Joint Future Operation Capability, as well as to the Joint Service Leader for Contamination Avoidance and most importantly to the Department of Defense. Fortunately, recent scientific work in biological spectroscopy at very high frequencies has suggested a novel avenue for a terahertz (THz) electronic approach to bio-warfare agent detection and identification (Woolard et al., 2001) and the extension of this work to practical sensing methodologies is the subject of this paper.

This paper discusses general issues and reports important results related to the practical application of terahertz-frequency absorption spectroscopy as a novel technique

for achieving standoff detection of bio-warfare agents. Transmission spectroscopy at THz frequencies (i.e., ~ 0.01-10 THz) has previously demonstrated applicability as a potential new technique for the detection and identification of biological agents. Indeed previous research results generated by our group have shown that due to a large number of unique resonance features that arise from phonon modes, the THz regime can be extremely useful for the study, analysis and identification of biological macromolecules under controlled laboratory conditions (Woolard et al., 2002). Here, detailed studies on DNA and complete cellular biological samples revealed detailed and high-level numerical structures possibly due to vibrational lattice and local phonon modes and other physical mechanisms of interactions between radiation and biological materials (Globus, Bykhovskaia et al., 2002, Globus, Woolard, et al., 2002).

The discovery of THz-spectral signature phenomenon was important to bio detection for a number of reasons. First, previous theoretical analysis has indicated that the resonant frequencies of such phonons within DNA material are strongly dependent on the weak hydrogen bonds of the double-helix base-pairs. Since all genetic information associated with living cells is encoded in the variety and arrangement of DNA nucleotides, this phenomenon suggested a promising mechanism for bio-agent detection because these phonons should be somewhat species specific. Second, this initial work demonstrated that a large number of species-specific phonon modes might be detected relatively easily from semi-dry films and that detection is enhanced by the orientation of the DNA fibers. These initial results indicated that the unique phonon signature for basic bio-molecules occurred at long-wavelengths in the THz frequency band. These investigations were subsequently extended to other relevant materials (e.g., RNA) and to complete cellular materials (e.g., bio-spores). Measurements demonstrated that spore materials (i.e., *Bacillus (B.) subtillus*) also contained similar spectral signature, which are most probably attributable to the protein molecules that make up most of the spore's protective shell. While the spectral resonance characteristics are quite weak (i.e., 5-15 % variations between local minimum and maximum), these results motivated a system design study to determine the sensitivity limits of various sensor architectures that utilized a differential-absorption-radar (DAR) remote-detection approach. This paper will assess and contrast the predicted system performance of incoherent (i.e., direct detection) and coherent DAR sensors applied towards the detection of aerosol bio-clouds. As these performance estimates utilize spectral signature data obtained from laboratory measurements on thin spore films, the issue of signature stability will also addressed. Finally, a demonstration methodology will be established to assess the utility of the DAR sensor for imaging the time-dependent evolution of an aerosol bio-cloud release. These results will demonstrate that standoff detection of bio-agents is feasible for threat-level concentrations in practical battlefield environments at sufficient ranges to provide for early warning.

2. DAR SYSTEM STUDY

This section will summarize results from design studies performed on differential-absorption radar (DAR) architectures that utilize active detection for sensing *B. subtillus* spore clouds. While passive schemes were consider in earlier studies (Brown et al., 2002), they were found to be too insensitive at the ranges (i.e., up to 1 km) and bioparticle concentrations (~ 10^3 cm^{-3}) due to the small absorption cross section of the typical spectral signature and the strong absorption by water vapor in the THz region. Alternatively, active sensors are potentially more sensitive than passive ones since they provide their own source of coherent radiation at a spectral density far above the background levels. The active DAR sensor considered here consists of a coherent transmitter operating minimally at two frequencies – one at the center of the absorption signature and one at the edge. By subtracting the received power alternately at the two frequencies, the absorption signature can be detected even in the presence of fluctuations in the atmosphere caused by wind and variable humidity. The technique is similar in principle to differential absorption lidar (DIAL) commonly used at IR wavelengths.

2.1 Absorption Signature Characteristics

An illustration of the type of absorption signature obtained from the DAR system is given in Fig. 1. Here, the system is measuring the power transmitted through a cloud of bioparticles at two hopping frequencies. While the background transmission in the THz region generally has a complex behavior, the bioparticle absorption typically introduces a broad "dip" in the transmission spectrum that is characterized by a minimum τ_{min} at frequency ν_{min} , a depth $\Delta\tau$, and a half-width $\Delta\nu$. $\Delta\tau$ is now defined as the absolute difference between τ_{min} and the background transmission τ_{back} measured at a frequency ν_{back} on whichever side of ν_{min} that τ is greater (e.g., in Fig. 1 $\nu_{back} >> \nu_{min}$). Hence $\Delta\nu \equiv |\nu_{min} - \nu_{back}|$. If the concentration of bioparticles, ρ, is assumed low enough that the attenuation can be described by a coefficient α

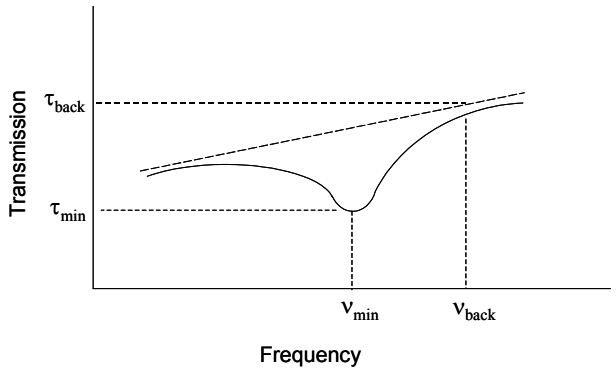

Fig. 1. Notional bioparticle absorption signature

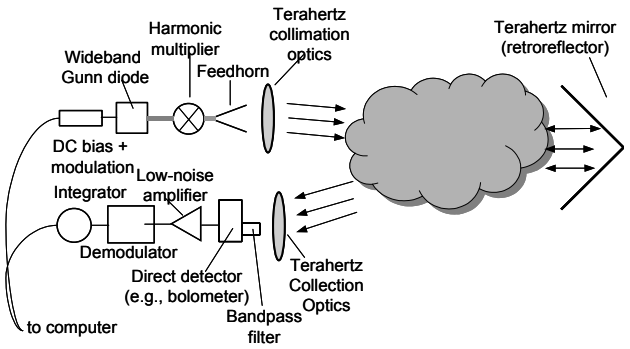

Fig. 2. Block diagram of sensor and target scenario.

that is linearly dependent on ρ then the transmission can be described by the Lambert-Beer law $\tau(\nu) = \exp[-\alpha_0(\nu)L\rho/\rho_0]$. In this expression L is the thickness of the bioparticle cloud and α_0 is a reference attenuation coefficient measured at a concentration ρ_0 that may be much different than the actual ρ. For the signature of Fig. 1 and assuming that the background transmission at each ν is constant one obtains

$$\Delta\tau \equiv \tau_{back}\{1-\exp[-\alpha_0(\nu_{\min})L\rho/\rho_0]\} \qquad (1)$$

Listed in Table I are the values of ν_{min} , $\alpha_0(\nu_{min})$, ν_{back} and $\Delta\nu$ derived from laboratory transmission measurements through dry films of *B. subtillus* containing $\rho_0 \approx 1\text{x}10^{12}$ cm^{-3} – a density that is necessary to get an accurate measure of $\Delta\alpha$, but is much larger than expected in airborne bio-warfare agents. The results listed in Table I describe five different absorption features having center frequencies between 327 and 1075 GHz. In the THz region, the remote detection of these signatures depends critically on the atmospheric transmission $\tau(\nu_{back})$.

Table I. THz absorption signatures of *B. Subtillus*			
Freq, ν_{min}	α_0 (ν_{min}) (cm^{-1})	ν_{back} , $\Delta\nu$ (GHz)	τ (ν_{back})
327 GHz	1.3	334.5, 7.5	0.008
421.5 GHz	0.7	430.5, 10.0	0.25
619.5 GHz	1.3	600.0, 19.5	$\sim 10^{-11}$
940.05 GHz	1.7	930.0, 10.05	$\sim 5\text{x}10^{-4}$
1075.5 GHz	1.2	1057.5, 18.0	$<10^{-30}$

2.1 Sensor-Target Scenario

The remote detection of bioparticles also depends critically on the scenario, which means the relative orientation of sensor and target, the physical size of the target, the optical depth of the absorbing species in the target, the atmospheric transmission between sensor and target, the background radiation, etc. For simplicity this analysis adopted the simple scenario shown in Fig. 2 consisting of a ground- or air-based active sensor looking into the sky at a target consisting of a cloud of dry bioparticles at temperature T_M and pressure P. Note here that the block diagram depicts an incoherent (i.e., direct) detection system. The cloud is assumed to have physical thickness L and to be located at a range R from the sensor. Behind the cloud is a retrodirective mirror that allows the transmitter and receiver to be co-located. The mirror is oriented relative to the sensor along a line-of-sight that cuts through a trajectory of length L through the cloud. The transmitter is assumed to radiate a constant power sequentially at the two frequencies ν_{min} or ν_{back} , defined in the previous section. This particular system conceptualization is amenable to either a perimeter-defense type system (i.e., with a stationary mirror) or a remote detection scheme where a small mirror could be mounted onto an unmanned airborne vehicle.

2.2 Atmospheric Transmission

Due to the strong propensity of bio-molecules to absorb radiation with the THz regime (i.e., with the same basic effect responsible for the bio-agent signatures), there exists a very high atmospheric attenuation from indigenous molecules that must be included in any realistic analysis of system sensitivity. In this study, a commercial radiative transport code, PCLnWin was applied which is based on the Fascode engine originally developed by the U.S. Air Force. The code solves for the radiation transmission as a function of slant angle and range for different model atmospheres in the presence of the common molecular species. Each absorption line is represented by the Voigt model with kinetic coefficients that account for pressure and Doppler broadening and that are fed into PcLnWin from the HITRAN96 database. The predominant absorber in the THz region is water vapor,

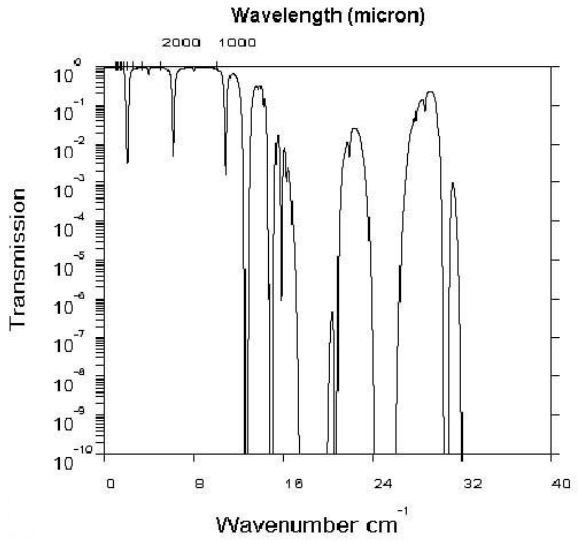

Fig. 3. Atmospheric Transmission computed by PCLnWin

which is better known for its lines at 22 and 183 GHz - the former having impacted radar history and the latter being the basis for atmospheric sounding radiometers. Also, several of the water lines in the THz region above 300 GHz are much stronger than these two. Fig. 3 shows the overall transmission spectrum computed by PcLnWin for a 1 km path at a slant angle of 5°, a relative humidity of 60%, and for the 7 atmospheric constitutents: H_2O, O_2, CO, CO_2, O_3, N_2O, and CH_4. Below 300 GHz the transmission is greater than 50% except at the strong water line and molecular oxygen band at 60 GHz. Above 300 GHz the water lines are so strong that with pressure broadening become opaque sub-bands through which atmospheric transmission is practically impossible. Fortunately, a few transmission windows persist, such as the ones around 400, 670, and 840 GHz. In analyzing the detectability of bioparticles it is important to consider the proximity of their signatures to these opaque sub-bands and transmission windows. Listed in Table I is the atmospheric transmission computed by PcLnWin for the 5 signatures of *B. Subtillus* at the line-center frequencies. Because of the high relative transmission ($\tau \approx 0.25$), the signature centered at 421 GHz has the best chance of being detected by an active remote sensor having practical levels of transmit power.

2.3 Sensor Simulation

This study considers both incoherent and coherent DAR sensing systems and the signal-to-noise ratio (SNR) performance and relative probabilities of detection and false alarm will be assessed for each. Of course, the distinguishing element between the two is that the incoherent DAR utilizes a direct-detection receiver (Rx) and the coherent system employs a Rx that operates by homodyne down-conversion. Whether an incoherent or coherent Rx is used, the DAR transmits alternately at two or more frequencies that span across the absorption signature as discussed earlier. Let us first consider the analysis of the incoherent DAR.

Incoherent DAR System Analysis

For the sensor architecture and scenario shown in Fig 2 and given the model of atmospheric propagation discussed above, the signal power at the receiver (Rx) can be estimated analytically given reasonable assumptions about the beam pattern of the transmitter (Tx). If one assumes that the lateral extent of the beam is much smaller than the cloud at the range where the beam passes through, then the received power can be related to the transmitted power P_T by the following (Friis) transmission expression where G_T is the gain of the Tx antenna, and A_R is the effective area of the Rx and R is the round-trip path length between. The R^{-2} dependence occurs in (2) instead of the usual R^{-4} radar factor because the retrodirective mirror is assumed to be perfectly specular. If we assume the Tx antenna is diffraction limited (easy to achieve in the THz region), then $G_T = 4\pi A_T/\lambda^2$, so that Eq. (2) can be written

$$P_R(\nu) = \frac{P_T A_T A_R \tau(\nu)}{R^2 \lambda^2} \tag{3}$$

The Rx noise power will generally be the sum of two terms: (1) background electromagnetic noise caused by fluctuations in the received power, and (2) electrical noise caused by fluctuations of various physical quantities in the electronic devices of the Tx or Rx. In the THz region, the background power is associated with blackbody radiation coming from the sky, the bioparticle cloud itself, or the optics, all of which are assumed to be at or near an ambient temperature of 290 K. At this temperature and in the THz region $h\nu/k_BT \ll 1$ ($k_B \equiv$ Boltzman's constant), hence, the Planck distribution for the blackbody radiation can be approximated in the Rayleigh-Jeans limit. Furthermore, if the Tx is radiating only a single frequency at a given time, then its power should be contained within one spatial mode. The Rx would then be optimally designed to receive just this mode, so that the received background power would be,

$$P_B \approx (4h\nu k T_B B/\eta)^{1/2} \tag{4}$$

where B is the RF bandwidth and η is the receiver coupling efficiency (Kingston, 1978). In a well-designed incoherent receiver, the electrical noise will be dominated by noise of the front-end direct detector. If we assign the

detector a noise-equivalent power of NEP_{det}, the overall receiver NEP can be written,

$$NEP_{rec} \approx (4h\nu kT_B B/\eta + NEP_{\det}^2)^{1/2} \quad (5)$$

Given the above expressions for the signal and noise, one can estimate the power S/N ratio of a direct receiver in baseband by including the effect of integration,

$$\frac{S}{N} \approx \frac{P_R}{NEP_{rec}} (2t_{\text{int}})^{1/2} \quad (6)$$

where t_{int} is the integration time. Substitution of (3) and (5) into (6) then yields

$$\frac{S}{N} \approx \frac{P_T A_T A_R \tau(\nu)(2t_{\text{int}})^{1/2}}{R^2\lambda^2 \left(4h\nu kT_b B/\eta + NEP_{\det}^2\right)^{1/2}} \quad (7)$$

To account for the change in Tx frequency that occurs in differential mode, we assume the Tx power remains constant and the duty cycle at each frequency is 50%. Hence the S/N is degraded by about a factor of two, and

$$\Delta P_R(\nu) = \frac{P_T A_T A_R \Delta\tau(\nu)}{R^2\lambda^2} \quad (8)$$

$$\left(\frac{S}{N}\right)_D \approx \frac{P_T A_T A_R \Delta\tau}{R^2\lambda^2} \frac{1}{(4h\nu kT_B B/\eta + NEP_{\det}^2)^{1/2}} \left(\frac{t_{\text{int}}}{2}\right)^{1/2} \quad (9)$$

Results from (9) have been computed for the sensor parameters listed in Table II and for three different concentrations of *B. subtillus*, ρ = 10, 10^3, and 10^5 cm^{-3},

Table II. Parameters used in sensor simulation	
Background temperature (K)	290
Detector coupling efficiency	0.5
Line center frequency (GHz)	421
Background frequency (GHz)	431
Linewidth (GHz)	10
Line center abs coeff (1/cm)	0.7
Background transmission	0.25
Spectral bandwidth (GHz)	10
Integration time (s)	1.0
Transmit power (mW)	1.0
Tx aperture (cm^2)	100
Rx aperture (cm^2)	100
Tx-Rx separation (m)	1000
Cloud thickness (cm)	variable
Cloud temperature (K)	290
Molecule density (cm^{-3})	$10,10^3,10^5$

that roughly span the interesting range for bio-warfare defense. The results are plotted vs. cloud depth in Fig. 4 for a fixed Tx-to-Rx separation of 1.0 km (0.5 km sensor to mirror). In Fig. 4 (a) the Rx detector is assumed to have NEP = $1x10^{-10}$ $W\text{-}Hz^{-1/2}$ corresponding to a state-of-the-art room-temperature bolometer (e.g., micro Golay cell). In Fig. 4 (b) the Rx detector is assumed to have NEP = $1x10^{-13}$ $W\text{-}Hz^{-1/2}$ corresponding roughly to a state-of-the-art cryogenic (4.2 K) bolometer (e.g., silicon composite). These results were used for quantifying

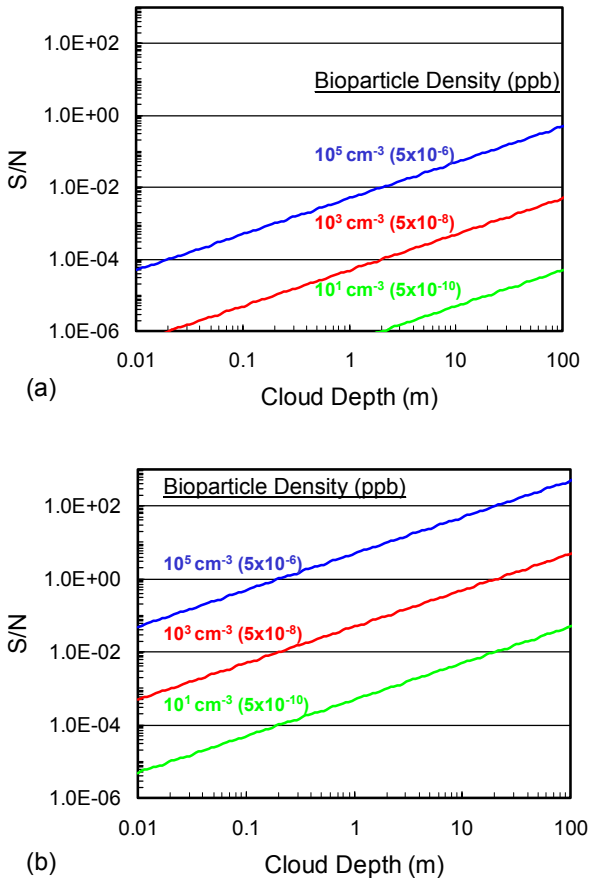

Fig. 4. SNR for NEP = (a) 10^{-10} and (b) 10^{-13} $W/Hz^{1/2}$

higher-level system metrics such as the minimum detectable concentration MDC (i.e., concentration where S/N=1) and the probabilities of detection, P_d, and false alarm P_{fa}. For example, according to Fig. 4 (b), in a cloud 20 m thick at a standoff of 0.5 km, the MDC is 10^3 cm^{-3}. Assuming that all noise mechanisms in the Rx are statistically Gaussian and setting the signal threshold at 0.2 nW, one finds Pd and Pfa values under these conditions to be approximately 0.4 and 0.1, respectively – unsatisfactory for most applications. However, the enhanced S/N at greater cloud depth in Fig. 4(b) allows for more reliable detection. For example, a cloud depth of 20 m and a concentration of 10^4 cm^{-3} yields a SNR of 10 and associated Pd and Pfa values of 0.75 and 0.006 if the threshold is increased to 0.9 nW. It is also possible to

increase the SNR significantly by utilizing an alternative transmitter sources (e.g., a tube source can easily provide over 10 times more power). However, as will now be shown, a coherent DAR directly provides for significantly better overall performance.

Coherent DAR System Analysis

In the *coherent* DAR the received power is multiplied against a portion of the transmitted power on a Schottky-diode mixer as illustrated in the block diagram of the system given in Fig. 5. This portion of transmitted power plays the traditional role of a local oscillator (LO). Aside from any small Doppler shift caused by the bioparticles, the LO and signal should have the same frequency, so the mixing process produces a difference-frequency (DF) power spectrum centered at dc. Hence this process, commonly called *homodyne* down-conversion, displays at least two important distinctions relative to an incoherent Rx. First, the multiplication amplifies the signal strength relative to the noise floor, generally yielding a superior SNR compared to the incoherent Rx. Second, because the phase of the received signal coheres to the demodulator input, the detection statistics are different.

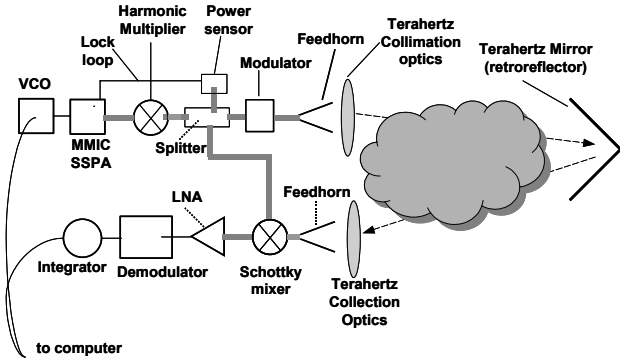

Fig. 5. Block diagram of coherent DAR system.

Analysis of the difference-frequency SNR, SNR_{DF}, in bioparticle DAR after the low-noise amplifier (LNA) leads to the curves shown in Fig. 6 (a). The transmit power is assumed to be 1 mW and the mixer is assumed to be driven hard enough (~1 mW) so that the noise-equivalent power (NEP) is limited by LO-shot noise and coupling losses to a value of $hf/\eta = 5.6\times10^{-21}$ W/Hz ($h \equiv$ Planck's constant) for f = 421 GHz and η = 5%. The DF bandwidth is assumed to be B_{DF} = 0.6 MHz. The bioparticle absorption characteristics and atmospheric transmission (~0.25) are the same as before for the incoherent DAR. To compare on equal footing to the incoherent DAR, we need to calculate the SNR after demodulation and integration ($t_i \equiv$ integration time). Such processing will, in the worst case, increase the SNR as the square-root of the number of received samples, so that the post-demodulation value $SNR_{PD} \approx SNR_{DF} \cdot (B_{DF}\ t_i\ )^{1/2}$. Assuming t_i = 1 ms we obtain the curves of SNR_{PD} shown in Fig. 6 (b). This SNR_{PD} is approximately 300 times larger than the analogous post-detection SNR of the incoherent Rx, which is approximately 1.0 under the conditions of the bullet in Fig. 6 (b).

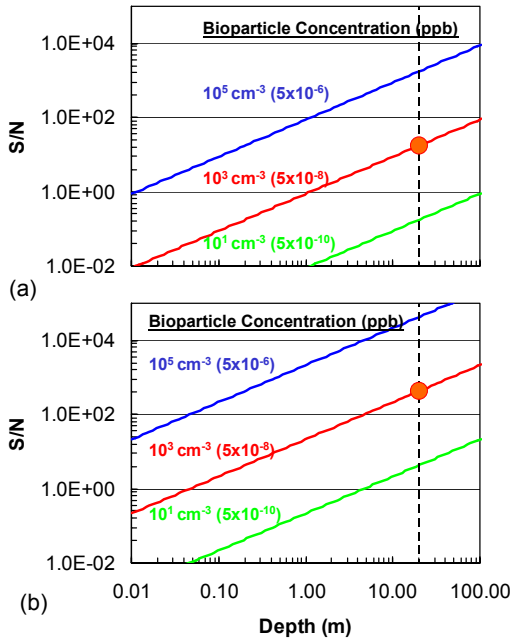

Fig. 6. (a) SNR_{DF} after LNA. (b) SNR_{PD} - Bullet defines point corresponding to incoherent DAR at SNR = 1.

The bioparticle-detection process is inherently a statistical issue that depends strongly on how the Rx combines the signal and noise samples from the demodulator and integrator. In this first-pass study we assume that the only source of noise is the Rx physical noise described above, and that only one sample is processed, which for the given B_{DF} of 1 MHz means the measurement interval is 1 μs. In this case the demodulator output (current) amplitude for noise-alone has Rayleigh statistics,

$$P_n(i) = (i / < i_n^2 >) \exp(-i^2 / 2 < i_n^2 >), \qquad (10)$$

and for signal-plus-noise has Rician statistics (Barton, 1988),

$$P_{s+n}(i) = (i / < i_n^2 >) \exp[-(i^2 + i_s^2) / 2 < i_n^2 >] I_0(i \cdot i_s / < i_n^2 >) \quad (11)$$

where i is the post-detection current, i_n is the DF noise current, i_s is the DF signal current , < > denotes time average, and I_0 is the modified Bessel function of order zero [2]. We then assume a post-detection threshold i_t to calculate the probability of false alarm,

$$P_{fa} = \int_{i_t}^{\infty} P_n(i) di = \exp(-i_t^2 / 2 < i_n^2 >) \qquad (11)$$

and the probability of detection

$$P_d = \int_{i_t}^{\infty} P_{s+n}(i)di \,, \tag{12}$$

where the latter is integrated numerically. The results of this analysis are plotted in Fig. 3. For example, under the conditions bulletized in Fig. 6 (a) for which the SNR_{DF} is 18, we find from Fig. 7 that $P_d \approx 0.99$ for $P_{fa} = 10^{-3}$, $P_d \approx 0.95$ for $P_{fa} = 10^{-4}$, and $P_d \approx 0.90$ for $P_{fa} = 10^{-5}$. These are, of course, just three points on a continuous P_d vs P_{fa} receiver operating characteristic (ROC) curve.

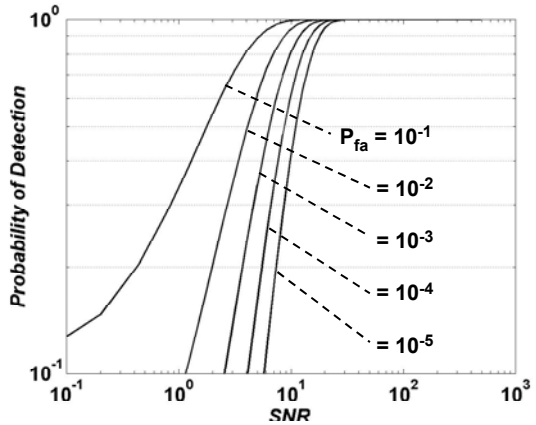

Fig. 6. (a) SNR_{DF} after LNA. (b) SNR_{PD} - Bullet defines point corresponding to incoherent DAR at SNR = 1.

3. SENSING SCIENCE

The DAR system performance estimates given in the last section make strategic use of THz-frequency spectral signatures that were derived from layered films of the *B. Subtillus* spores. In fact, the experimental data used to derive the differential transmission of *Bacillus subtillus* (which is a simulant for Anthrax) are illustrated in Fig. 7 for different amounts of material (i.e., layer thickness)

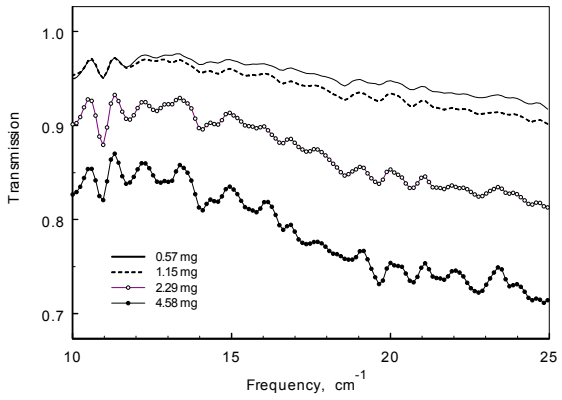

Fig. 7. Experimental transmission Spectra of *B. Subtillus*.

and show very good scaling characteristics. These particular results are useful in quantifying a remote sensor because *B. Subtillus* is a surrogate of the actual warfare agent threat Anthrax. Obviously, the magnitude of the differential absorption (DA) is the leading factor that determines the final sensitivity of the DAR sensor. Hence, an accurate estimate of DA is important for reliable predictions of performance. It is also very important to note that the bio-materials are inherently fragile and that their molecular conformation and spectral characteristics are strongly influenced by environmental factors. In fact, the resonance features in the spectra can be more or less pronounced depending on the quality of material, sample preparation and measurement conditions. For example, the mode coupling strength can be affected by the polarization of the electromagnetic field in relation to the dipole moment of the DNA oscillators (Globus, Woolard, et al, 2002). Thus sample rotation and the polarization level of the source can affect the predicted DA used in these studies Even more importantly, films of uniform thickness are well known to exhibit interference fringes in their reflection and transmission spectra. These interference phenomena can obscure fine resonance features or be misinterpreted as modes themselves Therefore a high level of expertise must be exercised to understand these effects and to differentiate them from the measured mode structure.

It is true that actual experimental measurements of bio-aerosols can be utilized to extract the data needed to assess the DAR system. Indeed, such a research project is actively being pursued under the ARO STTR program. However, this is a costly and time-consuming endeavor and one that can not easily provide fundamental insight for the potential control and enhancement of the spectral features. These facts have motivated our group to pursue detailed scientific investigations into the spectral characteristics of molecules of know composition and structure. Here, the goal is to develop physics-based insights for predicting the level of signature instability and for identifying signature enhancement techniques. For example, Figs. 8 (a) and (b) illustrate the importance of interference effects and sample orientation relative to the electric (E) field that were obtained from studies on 160 μm thick, free-standing films of Poly [A] and Poly[A]-Poly[U] RNA, respectfully. Fig. 8 (a) gives spectra taken from Poly [A] samples with highly orientated structure and high sensitivity and good reproducibility was achieved even though a strong fringing envelope (which tends to obscure some phonon modes) is present for these relatively thick samples. Fig 8 (b) gives results for Poly[A]-Poly[U] samples where the rod-like polymers were only partially aligned and where the measurements were performed at two different orientations to the E-field. Here, the very thin samples exhibit virtually no interference pattern but show a very strong dependence on sample rotation. Such a polarization effect could not be produced by an "etalon" effect and is direct evidence that the spectral characteristics arise from microscopic

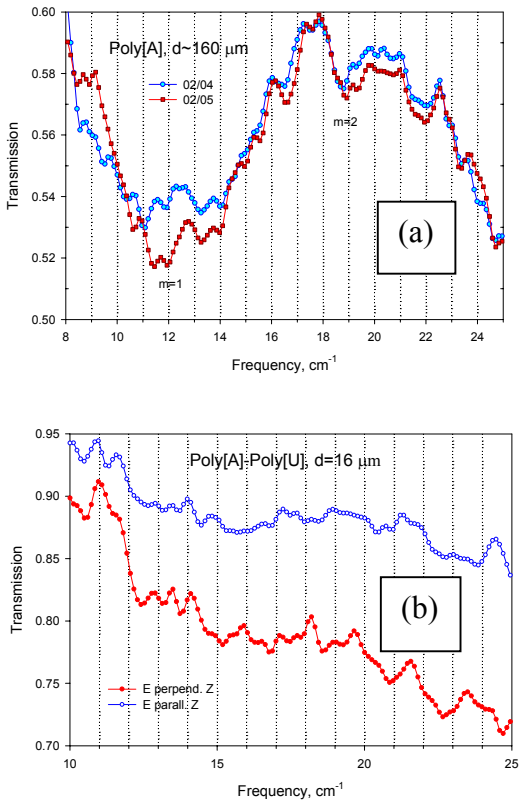

Fig. 8. Spectra for (a) Poly[A] and (b) Poly[A]-Poly[U].

processes (e.g., phonon modes) within the biological material. Furthermore, the observation that resonance structure is more pronounced at this orientation correlates with the higher oscillator strengths, as was predicted by our earlier modeling results (Globus, Bykhovskaia et. al., 2002). These scientific investigations into the microscopic properties of molecules are more important than may be immediately apparent since it has been previously demonstrated (Woolard, Globus, et al., 2000) that even spores can exhibit non-symmetric structure behavior that influences the THz spectra.

4. BIO-AGENT ATTACK SENARIO

A complete assessment of DAR sensor performance can only be achieved by considering its implementation within a realistic bio-agent attack scenario. Specifically, to this point in the study the sensitivity of the DAR system has been derived for a single line-of-sight (LOS) measurement. Of course, this is adequate if one were interested in deploying a DAR monitor that would provide a perimeter-defense around a controlled area (i.e., where one could establish points for the Tx/Rx unit and the mirror). However, if the goal is the monitoring of bio-clouds at a distance (i.e., where a mirror must be deployed to a point opposite the cloud) then the issue of sensitivity over the field-of-view (FOV) for the cloud (i.e., how much of the cloud can you image) and how that varies as a function of time (i.e., how long can you see the cloud) become very important. This is important because it will define how many mirrors are required to provide the adequate levels for P_d and P_{fa} over the entire battle-space. This issue is being addressed through the incorporation of data generated for a biological attack scenario. Here, numerical maps of bio-agent density time-dependent evolution are simulated using the VLSTRACK computer model. LOS trajectories are then defined from the perspective of the sensor and they are then used to derive the effective bio-density for the transmission path. This allows for mapping the system probability statistics over the user FOV and demonstrates the utility of the system on the battlefield. These results are to be presented at the conference meeting.

5. CONCLUSIONS

Detailed design studies were presented for a differential-absorption-radar (DAR) approach that utilizes the spectral signatures of *Bacillus (B.) subtillus* spores within the terahertz (THz) regime as the detection mechanism. These results demonstrate that THz DAR standoff detection of bio-agents is feasible for threat-level concentrations in practical battlefield environments at sufficient ranges to provide for early warning.

REFERENCES

Brown E.R., Woolard D. L. et al., "Remote Detection of Bioparticles in the THz Region," in proceedings to the IEEE 2002 IMS, Seattle, WA, June 2002.

Globus T., Woolard D., et al., "Submillimeter-Wave FTIR Spectroscopy of DNA Macromolecules and Related Material," *J. of Appl. Phys.* Vol. 91, pp. 6106-6113, 2002.

Globus T., Bykhovskaia M., et al., "Submillimeter-wave Spectral Signatures of Artificial RNA Molecules," invited to *J. of Appl. Phys*. D, 2002.

Kingston R. H., *Detection of Optical and Infrared Radiation,* (Springer, New York, 1978).

Woolard, D., "Terahertz Electronics Research for Defense," in the proceedings to the 2000 Space THz Conf., U. of Michigan , 2000.

Woolard D., Globus, T., et al., "The Potential Use of Submillimeter-Wave Spectroscopy as a technique for Biological Warfare Agent Detection." in proceeding to 22nd Army Science Conf., 2000.

Woolard, D., et al. "Sensitivity Limits & Discrimination Capability of THz Transmission Spectroscopy for Biological Agent Detection" in proceedings to Joint Conf. On Standoff Detection for CBD, Sept., 2001.

Woolard, D., Globus, T., et al., "Submillimeter-Wave Phonon Modes in DNA Macromolecules," *Phys. Rev. E,* Vol. 65, 051903, May 2002.